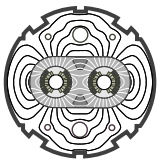

LHC Project Note 314

February 26, 2003
Jorg.Wenninger@cern.ch

Determination of LHC Main Dipole Field Errors during a Sector Test using Trajectory Analysis

J. Wenninger

Keywords: Sector test, Field harmonics, Trajectory

Summary

During the installation phase of the LHC, a beam test of a complete LHC arc may be performed in the year 2006. One of the motivations for such a test is the experimental determination of the field errors of the main dipole magnets directly with beam. The possibility of obtaining useful information on certain field errors from an analysis of the trajectory response to orbit corrector kicks has been evaluated. The influence of monitor noise and calibration errors has been tested. This first study indicates that under the conditions that have been evaluated, it is possible to determine the average a_2, b_2 and b_3 field errors of the main dipoles and the average b_2 field error of the main quadrupoles and perform a check of the test bench measurements of the magnets during the sector test.

1 Introduction

The installation of the LHC machine in the former LEP tunnel will take place between 2004 and the end of 2006. During that period the eight sectors (or arcs) will be installed and commissioned one after another. In 2006 it will be possible to inject low intensity beam into sector 8 to 7. Besides providing a system check for many elements, in particular beam position and beam loss monitors, this test may also allow to verify the field quality of the LHC magnets directly with beam. Since during such a sector test the only diagnostics is obtained through trajectory measurements of approximately 50 beam position monitors in each plane, the effects of the field errors must be sufficiently large to be detectable from a single pass trajectory measurements.

This note first describes a procedure to extract information on a machine model from trajectory or closed orbit analysis based on the LOCO program [1]. The data analysis procedure is then applied to simulated LHC trajectories including the effects of magnetic field errors,of monitor noise and of calibration errors.

2 Orbit Response Analysis

The analysis of the machine optics in terms of orbit response is based on the relation between the beam position measured at the location of N beam position monitors (BPM) represented by a vector $\vec{u}$

$$\vec{u} = \begin{pmatrix} u_1 \\ u_2 \\ ... \\ u_N \end{pmatrix} , \tag{1}$$

and a set of M dipole magnets (correctors) deflections (kicks) represented by a vector $\vec{\theta}$

$$\vec{\theta} = \begin{pmatrix} \theta_1 \\ \theta_2 \\ ... \\ \theta_M \end{pmatrix} . \tag{2}$$

Orbit position and corrector deflections are related by a response matrix $\mathbf{R}$ (dimension $N \times M$),

$$\vec{u} = \mathbf{R}\vec{\theta} . \tag{3}$$

The element R_{ij} of the response matrix corresponds to the orbit shift at the i^{th} monitor due to a unit kick from the j^{th} corrector. For a linear optics, matrix $\mathbf{R}$ does not depend on the kick strength, respectively orbit amplitude, and element R_{ij} is given by

$$R_{ij} = \frac{\sqrt{\beta_i \beta_j}\cos(|\mu_i - \mu_j| - \pi Q)}{2\sin(\pi Q)} \tag{4}$$

for a closed orbit and by

$$R_{ij} = \begin{cases} \sqrt{\beta_i \beta_j}\sin(\mu_i - \mu_j) & \mu_i > \mu_j \\ 0 & \mu_i < \mu_j \end{cases} \tag{5}$$

for a trajectory. β and μ are the betatron function and phase advance, Q is the machine tune. Matrix $\mathbf{R}$ holds a large amount of information about the machine optics, albeit in a complex and highly entangled form. On the other hand, $\mathbf{R}$ can be determined easily and in a non-destructive way.

The LOCO program [1] is a fit program that is designed to match a measured orbit response matrix of a ring or line with the machine model while properly taking into account the monitors and orbit corrector calibration errors. Orbit corrector and BPM roll angles can also be determined. LOCO has been used in various places, including the SPS where problems with the horizontal orbit correctors, most likely inter-turn shorts, were discovered with the help of LOCO [2].

2.1 LOCO Analysis Principle

To use the information contained in the response matrix, the first step consists in building the vector $\vec{V}$ obtained by the difference between the measured and the modelled response

matrix. The elements of this vector are

$$V_k = \frac{R_{ij}^{meas} - R_{ij}^{mod}}{\sigma_i} \qquad \forall i, j \tag{6}$$

where σ_i is the measurement noise of the i^{th} monitor. The norm of vector $\vec{V}$ represents the normalized error of the machine model with respect to the measurement.

The goal of the fit procedure is to minimize the norm of vector $\vec{V}$ (and therefore of the difference between model and measurement)

$$\|\vec{V}\|^2 = \sum_{k=1}^{N} V_k^2 = \text{minimum} \; . \tag{7}$$

by adjusting N_f fit parameters related to the machine model, to the monitors and to the orbit correctors. For correctly evaluated Gaussian errors, $\|\vec{V}\|^2$ should be distributed according to a χ^2-distribution. The expected minimum value for $\|\vec{V}\|^2$ is given approximately by the number of elements of $\vec{V}$ minus the number of fit parameters. The value of the minimum provides a statistical test of the fit quality and of the correct assessment of the BPM errors. A minimum value that is too low (high) indicates that the errors σ_i are over(under)-estimated.

To perform a fit of the response, N_f parameters c_l must be selected, and the dependence of each element of vector $\vec{V}$ on each parameter c_l must be evaluated. The resulting sensitivity matrix $\mathbf{S}$ with elements S_{kl} defined by

$$S_{kl} = \frac{\partial V_k}{\partial c_l} \tag{8}$$

can be used to approach the solution of the minimization by linearizing the problem. The three main categories of parameters are :

- BPM calibration factors, where $S_{kl} = -R_{ij}^{mod}/\sigma_i$.
- Corrector calibration factors, where $S_{kl} = R_{ij}^{mod}/\sigma_i$.
- Optics model parameters (magnetic strengths, elements misalignments...). For such parameters, the sensitivity must be evaluated with a modelling program like MAD [3] using a linear approximation

  $$S_{kl} = \frac{R_{ij}^{mod}(c_l + \delta c_l) - R_{ij}^{mod}(c_l)}{\delta c_l \; \sigma_i} \tag{9}$$

  where the response matrix change must be evaluated for a selected increment δc_l of each parameter. Equation 9 corresponds to the local fit gradient and the increment must be chosen carefully.

The norm of vector $\vec{V}$ is minimized iteratively by solving the linear equation

$$\vec{V} + \mathbf{S}\Delta\vec{c} = 0 \tag{10}$$

for the increment $\Delta\vec{c}$ in the parameter vector $\vec{c}$. This equation is identical to the equation that must be solved for orbit corrections (Equation 3), we can therefore apply the usual least-square algorithms (SVD [4], MICADO [5]) to solve for $\Delta\vec{c}$. Once a new value of $\vec{c} \rightarrow \vec{c} + \Delta\vec{c}$ is obtained, the procedure must be iterated and the model and vector $\vec{V}$ updated. In particular, the sensitivity matrix (Equation 8) must be re-evaluated around the new optimum and Equation 10 must be solved again. This procedure is iterated until a stable solution is found, i.e. when $\Delta\vec{c} \simeq 0$.

It is important to note that matrix $\mathbf{S}$ is actually rank deficient (i.e. 'singular') : there are an infinite number of solutions obtained by multiplying both the orbit corrector strength and the orbit change by the same factor. For this reason it is not possible to determine the absolute calibration of orbit monitors or corrector magnets from the response matrix alone. For the horizontal plane the absolute scale can be obtained by a known energy change over the RF frequency. The radial movement can be used to calibrate the absolute scale of the horizontal monitors.

Because of the singular nature of matrix $\mathbf{S}$, Equation 10 is solved using the Singular Value Decomposition algorithm [4]. The SVD algorithm is a powerful tool to handle singular systems and to solve them in the least square sense. For a matrix $\mathbf{S}$ of dimension $n \times m$ with $n \geq m$ the singular value decomposition has the form

$$\mathbf{S} = \mathbf{U}\mathbf{W}\mathbf{V}^{\mathbf{T}} = \mathbf{U} \begin{pmatrix} w_1 & 0 & ... & 0 \\ 0 & w_2 & & \\ ... & & ... & 0 \\ 0 & ... & 0 & w_m \end{pmatrix} \mathbf{V}^{\mathbf{T}} \,, \tag{11}$$

where $\mathbf{W}$ is a diagonal $m \times m$ matrix with non-negative diagonal elements. $\mathbf{V}^{\mathbf{T}}$ is the transpose of the $m \times m$ orthogonal matrix $\mathbf{V}$,

$$\mathbf{V}\mathbf{V}^{\mathbf{T}} = \mathbf{V}^{\mathbf{T}}\mathbf{V} = \mathbf{I} \,, \tag{12}$$

while $\mathbf{U}$ is an $n \times m$ column-orthogonal matrix

$$\mathbf{U}^{\mathbf{T}}\mathbf{U} = \mathbf{I} \,. \tag{13}$$

The least-square solution to Equation 10 is

$$\Delta\vec{c} = \mathbf{V}\mathbf{W}^{-1}\mathbf{U}^{T}\ \vec{V} \tag{14}$$

where $\mathbf{W}^{-1}$ is the 'inverse' of matrix $\mathbf{W}$, with all singular elements $1/w_k > 1/\epsilon$ set to 0. $\epsilon > 0$ is a selected cut-off value that can be adapted for each data set depending in particular on input conditions (noise...).

For a machine with N BPMs and M corrector magnets *per plane*, the size of matrix $\mathbf{S}$ is

- $(2 \times N \times M) \times (2 \times (N+M) + N_f)$ if the coupling terms between the planes are ignored,
- $(4 \times N \times M) \times (2 \times (N+M) + N_f)$ if the coupling terms are included,

since the number of parameters must a priori include the calibration factors of all BPMs and correctors $(2 \times (N+M))$. The matrix size grows rapidly for large machines. For the SPS,

$N \cong 120$ and $M \cong 110$, and $\mathbf{S}$ has dimensions $26'400 \times 460$. For the LHC, $N \cong 500$ and $M \cong 280$, and $\mathbf{S}$ has dimensions $\sim 280'000 \times 1'600$. While for the SPS the entire ring can still be handled, it is essentially impossible to handle matrices of the size required for the LHC. In practice the problem can of course be split into smaller 'problems' by using only a subset of the orbit correctors or orbit monitors.

2.2 The LOCO Software

LOCO consists in a collection of FORTRAN programs to fit the orbit response and generate automatic MAD scripts at each iteration. The original program has been slightly modified and the following features have been added and changed.

- The possibility to use BPMs that measure only a single plane (horizontal or vertical) has been added, mainly for the SPS and the transfer lines.
- The MAD script generation has been improved to handle transfer lines (or single turn trajectories) as well as rings.
- An automatic rejection of BPMs with gain factors that are outside tolerances (typically below 0.25 and above 2.5) has been added.
- The possibility to re-normalize the corrector and BPM calibrations by a common scale factor between to iterations.
- A program was added to generate simulated measurements as input to LOCO. This program reads MAD output data and re-formats the data to be suitable for LOCO. The user has the possibility to add BPM noise, BPM calibration factors and corrector strength errors to generate realistic input data for LOCO. This program was used for the present study to generate the input data for the simulated fits starting from trajectories generated with MAD.

3 Response Simulations and Fits

3.1 Magnetic Field Expansion

The magnetic field expansion used for the LHC is [6]

$$B_y + iB_x = B_{ref} \sum_{n=1}^{\infty} (b_n + ia_n)(\frac{x+iy}{R_{ref}})^{n-1} \tag{15}$$

where subscript $n = 1$ refers to a dipole, $n = 2$ to a quadrupole field and so on. The terms a and b correspond to the skew and normal harmonics. B_{ref} represents the reference magnetic field at the reference radius R_{ref} of 17 mm. For each harmonic the field error can be split into a systematic component that is identical for all magnets of the ring or of a sector and into a random component that varies from one magnet to the next. The field errors can be due to geometric effects, to persistent currents or induced by the ramp. A detailed description can be found in Reference [7]. In our case, only geometric and persistent current errors are

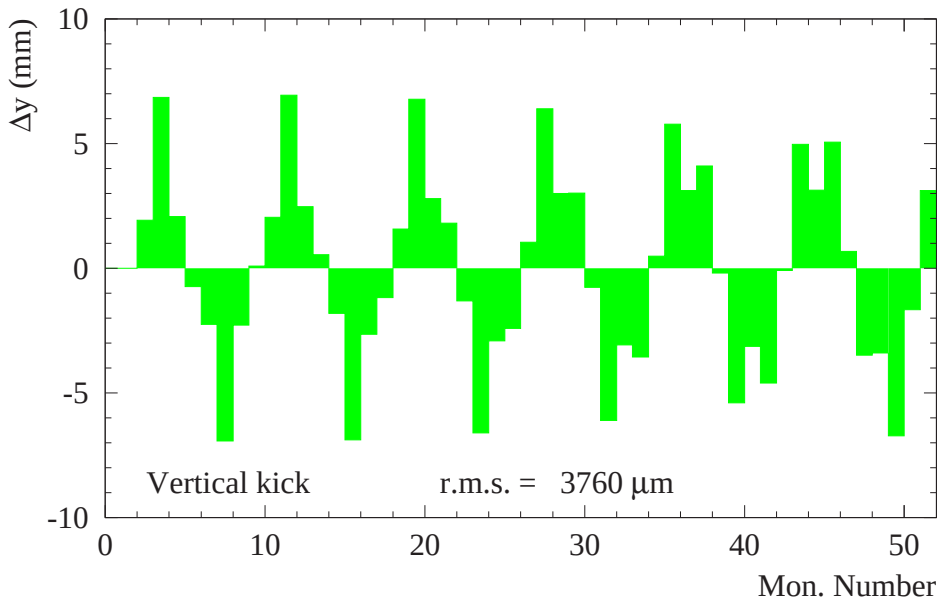

Figure 1: Example of the trajectory over one arc due to a 40 μrad kick of a vertical orbit corrector at the beginning of the arc, for a machine without any field errors in the main dipoles and quadrupoles.

of interest. In the LHC convention *one unit* of field harmonic corresponds to $b(a)_n = 10^{-4}$, and this unit will be used throughout this document for all field errors.

3.2 Simulation Input

The simulations were performed for arc 2-3 of LHC ring 1, which is in principle equivalent to arc 8-7 of LHC ring 2 but simpler and faster to run within MAD. In any case the results should not differ significantly between arcs. The machine model is based on a MAD8 V6.2 thin lens model. Field errors are generated and applied with the standard LHC MAD scripts.

The simulations are based on 12 horizontal and 12 vertical kicks of 30 μrad each using the correctors in the first half of a sector. The horizontal orbit corrector range starts with corrector MCBCH6.R2B1 and ends with corrector MCBH30.R2B1. For the vertical plane the corrector range is MCBCV7.R2B1 to MCBV29.R2B1. Another identical set was included with kicks of 40 μrad using the same orbit correctors, giving in total 48 different responses. 52 BPMs were used in each plane, from BPM.10R2.B1 to BPM.7L3.B1. For kicks of 40 μrad the maximum trajectory excursions reach approximately 8 mm. Such excursions should be just acceptable for single passage provided the emittance of the beams is close to nominal value. An example of a trajectory over one arc is shown in Figure 1 for a vertical kick of 40 μrad at the beginning of the arc.

The choice of monitors and correctors has not been optimized, but corresponds to a first guess. The two different kicks strengths are used to help separate effects from linear (a_2 and b_2) and non-linear (a_3, b_3 and higher) errors. In the event of a test with beam, a significantly

larger data set should be acquired to obtain the largest possible amount of information. The main aim of the selection of responses used here is to evaluate if a measurement is at all meaningful.

In practice, the trajectory (or orbit) responses are obtained from the difference of two measurements, one without kick (the reference) and one with a kick. Obviously it is possible to record more than one trajectory for each case and calculate an average to reduce the effects of various noise sources. For a reference trajectory that is well corrected and with an r.m.s. that is significantly smaller than the r.m.s. change due to the corrector kicks, the situation is roughly comparable to a situation of a perfectly centered trajectory. For that reason, alignment errors as well as b_1 and a_1 field errors have not been included in the simulations at this stage.

3.3 Trajectory Response and Field Harmonics

The effect of the main harmonic field errors of the dipoles, namely b_2, a_2 and b_3 is shown in Figures 2 to 4. The errors include the geometric and persistent current contributions and are generated according to error table 9901 [7]. Both systematic and random field errors are included.

Of particular interest is the b_3 harmonic which affects the machine chromaticity. The effects of the expected b_3 field error in the main dipoles (MB) are shown in Figures 3 and 4 for orbit correctors deflections of 40 μrad. The horizontal and vertical magnetic fields due to a b_3 component are

$$B_x(x,y) = \frac{2B_{ref}b_3}{R_{ref}^2}xy \tag{16}$$

and

$$B_y(x,y) = \frac{2B_{ref}b_3}{R_{ref}^2}(x^2 - y^2) \tag{17}$$

where x and y are the horizontal and vertical coordinates of the beam.

For a horizontal trajectory excursion, $B_x = 0$ while $B_y \propto x^2$ has always the same sign, leading to a systematic horizontal orbit shift visible in Figure 3, top plot. For a vertical trajectory excursion, $B_x = 0$ while $B_y \propto y^2$ has always the same sign, leading to a systematic coupled horizontal orbit shift visible in Figure 3, bottom plot.

The trajectory changes due to b_2, a_2 and b_3 are sufficiently large and different in their pattern that they should be disentangled by a fit. The effect of the a_3 component is too small to be detectable.

The effect of b_2 field errors in the main quadrupoles (MQ) is shown in Figure 4. The effect is significantly smaller than the expected b_2 component of the main dipoles, but as will be shown later, it can be separated from the effect of the dipoles. All other field errors of the main quadrupoles are too small to be detected in a realistic situation with BPM noise and calibration errors.

3.4 Monitor Noise and Calibration Errors

For all cases displayed in Figures 2 to 4, the r.m.s. trajectory changes are rather small, and can easily be hidden by large BPM noise or large calibration errors. Since the expected

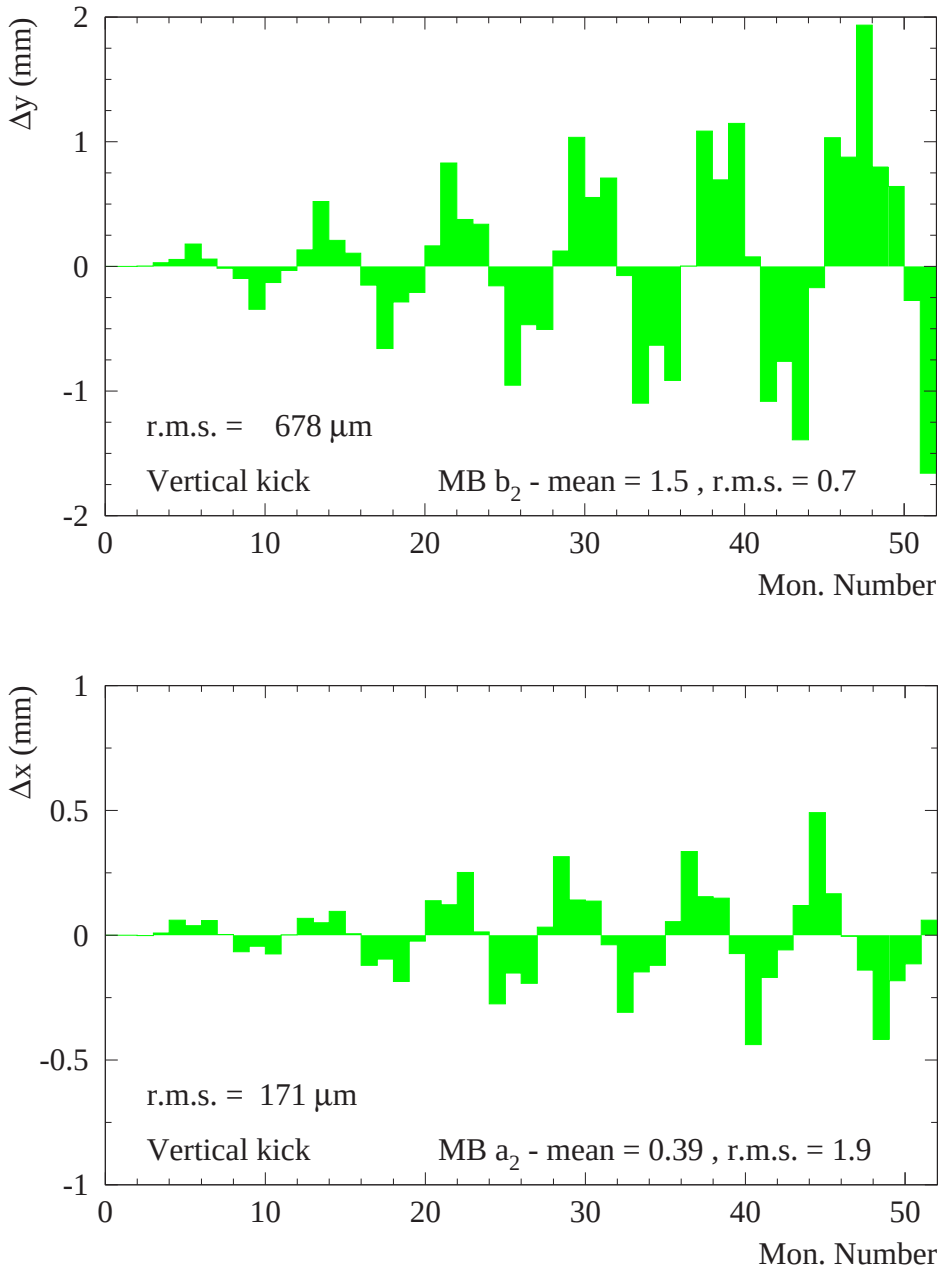

Figure 2: Change of the trajectory displayed in Figure 1 due to the influence of field errors. Top : vertical trajectory change due to typical b_2 field errors of the main dipoles, with a mean value of 1.5 units and a r.m.s. over the arc dipoles of 0.7 units. Bottom : horizontal trajectory change due to a_2 field errors of the main dipoles, with a mean value of 0.4 units and a r.m.s. over the arc dipoles of 1.9 units.

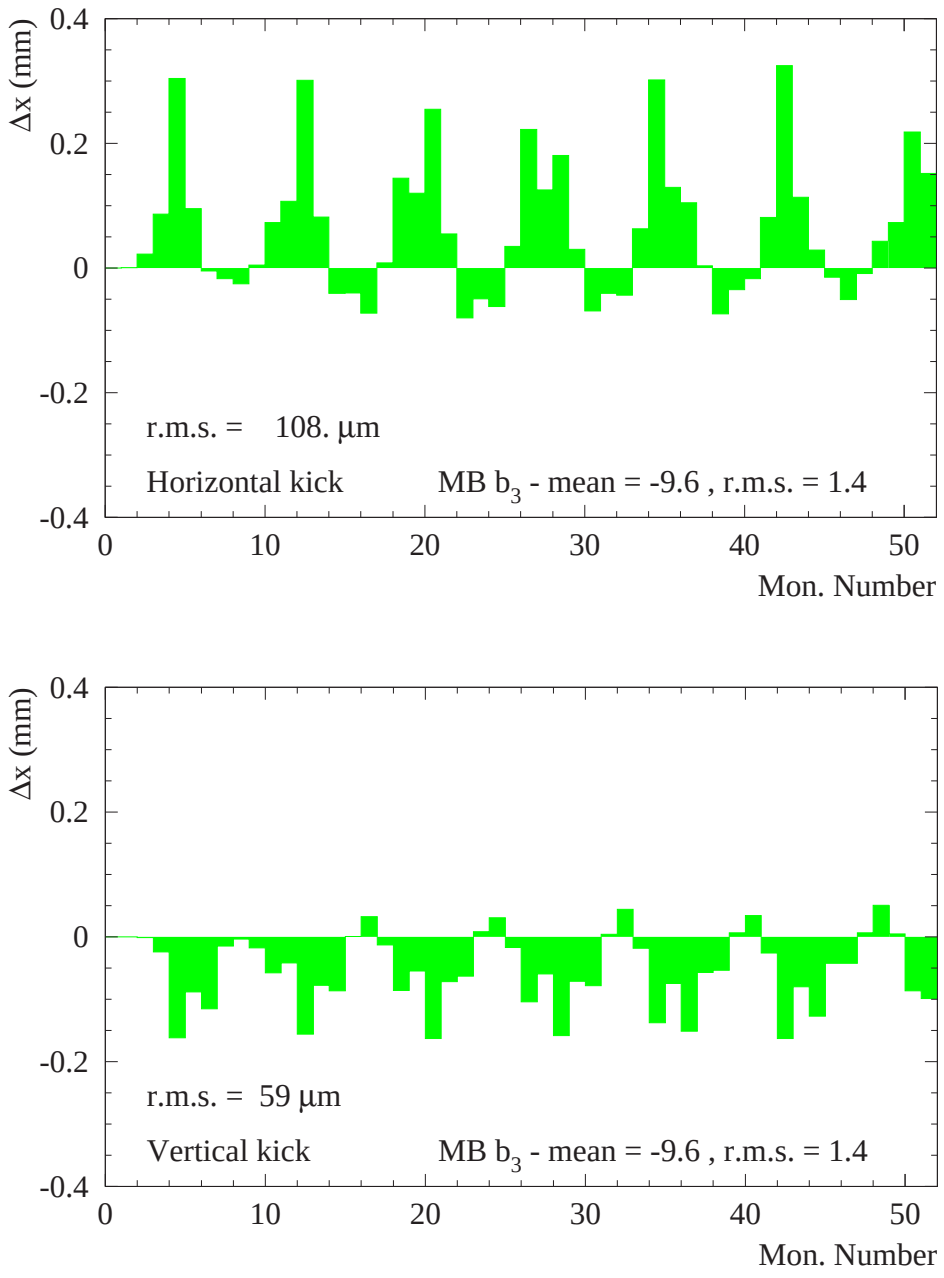

Figure 3: Effect of b_3 field errors of the main dipoles, with a mean value of -9.6 units and a r.m.s. over the arc dipoles of 1.4 units. Top : horizontal trajectory change for a horizontal kick of 40 μrad. Top : horizontal trajectory change for a vertical kick of 40 μrad (Figure 1).

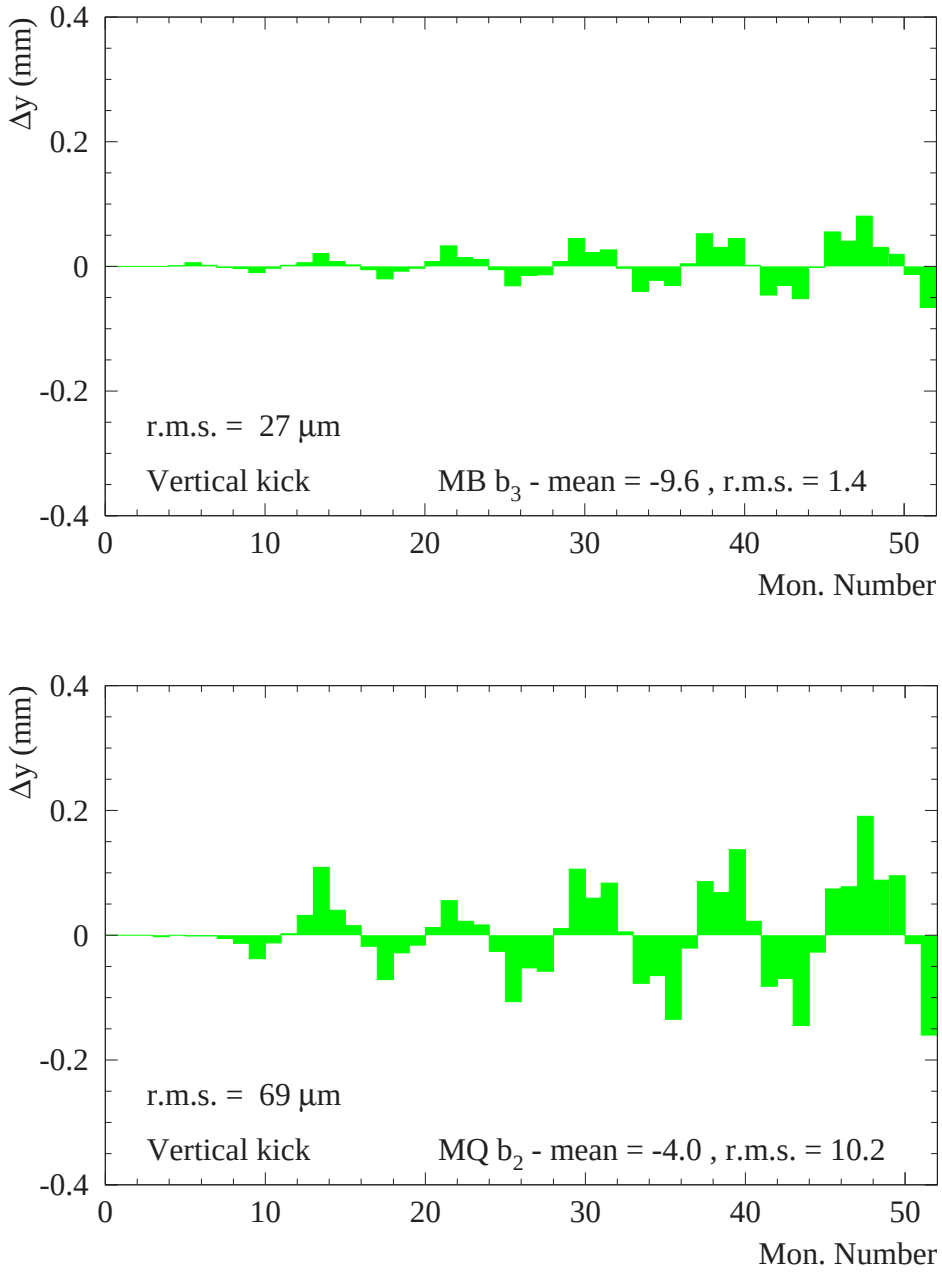

Figure 4: Change of the trajectory displayed in Figure 1 due to the influence of field errors. Top : vertical trajectory change due to b_3 field errors of the main dipoles, with a mean value of -9.6 units and a r.m.s. over the arc dipoles of 1.4 units. Bottom : vertical trajectory change due to b_2 field errors of the main quadrupoles, with a mean value of -3.9 units and a r.m.s. over the arc quadrupoles of 10.2 units.

Field errors		$f^{fit} - f^{mod}$ in standard units		BPM noise	Calibration errors (%)		$\|\vec{V}\|^2$
Magnet	Component f	average	r.m.s.	(μm)	BPMs	Corr.	
MB	b_2	$+0.00 \pm 0.01$	0.05 ± 0.01				
MB	b_3	-0.01 ± 0.09	0.40 ± 0.06	25	0	0	~ 6800
MQ	b_2	-0.36 ± 0.28	1.26 ± 0.20				
MB	b_2	$+0.00 \pm 0.01$	0.06 ± 0.01				
MB	b_3	-0.14 ± 0.13	0.58 ± 0.09	50	1	0.1	~ 5400
MQ	b_2	$+0.27 \pm 0.24$	1.08 ± 0.17				
MB	b_2	$+0.00 \pm 0.01$	0.06 ± 0.01				
MB	b_3	$+0.14 \pm 0.10$	0.43 ± 0.07	100	4	0.2	~ 5000
MQ	b_2	$+0.01 \pm 0.30$	1.34 ± 0.20				

Table 1: Fit of the b_2 components of the dipoles and quadrupoles and of the b_3 component of the main dipoles for different input conditions on noise and calibration errors. The model of the machine used for those simulations included only the b_2 and b_3 components of the main dipoles and quadrupoles, generated according to error table 9901. 20 seeds were generated for each case.

noise for a trajectory measurement is estimated to be $\simeq 50$ μm for a single bunch of nominal intensity with 10^{11} protons [8], the BPM noise was varied in the simulation between 25 and 200 μm. The BPM calibration errors were varied between 0 and 4%, the later value being typical for SPS position monitors but may be somewhat pessimistic for the LHC monitors. For the orbit correctors, the strength errors were varied between 0 and 0.2%.

So far no errors were included to simulate injection oscillations or BPM roll angles.

3.5 Fit Results

Each LOCO fit includes 104 orbit monitor calibration factors (52 per plane) as well as 48 orbit corrector calibration factors, since a different factor is assumed for the two kick strengths to account for possible hysteresis effects or calibration table errors. In addition to those 152 basic parameters, between 3 and 4 different field errors were also included in the fits.

In a first step, the machine model was set up to include only b_2 and b_3 field errors in the main dipoles and quadrupoles, generated according to error table 9901. The field errors used in the fit included the average b_2 and b_3 errors of the main dipoles and the average b_2 error of the main quadrupoles. The effect of the b_3 field error of the quadrupoles is too small and the fit turned out to be insensitive to this parameter. Fit results are given in Table 1 for different BPM noise conditions and calibration errors. No systematic bias is observed on the fitted field errors, and the r.m.s. differences between fit and input values are sufficiently small to yield interesting information. The b_3 error of the MB is determined with a precision of $\sim 0.4 - 0.5$ units for a mean value of ~ -9.5 units. The influence of noise and calibration errors are small : no important change is observed in the r.m.s. spreads between the best and the worst conditions. For a good fit, $\|\vec{V}\|^2$ should be $\leq 4900 - 5000$, a value that is reached for noise of 100 μm. With small BPM noise, the random field errors

contribute significantly to the difference between fit model (which does not include random components) and measurement and increase the achievable minimum value of $\|\vec{V}\|^2$.

In a second steps all field errors (normal and skew) of orders 2 to 5 were included in the machine model. The average a_2 field error of the main dipoles was added as fit parameter. Results are given in Table 2. The correlations between model input and fit results are shown in Figures 5 and 6 for the case where the BPM noise is 50 μm and the BPM calibration errors are 1%. The average fit value for the a_2 and b_2 components of the main dipole give good results. As expected, the additional random components compared to the situation with only b_2 and b_3 errors contribute to the measurement noise and degrade the fit quality for small noise. The error on the b_3 component of the dipoles is degraded by almost a factor two when the additional terms are included, compare Tables 1 and 2. The quality of the quadrupole b_2 component is also degrading, in particular a systematic shift of the fit result seems to appear. Furthermore, there is now a rather clear increase in the spread between input and fit values for the quadrupole b_2 field error as the noise is increased.

Field errors		$f^{fit} - f^{mod}$ in standard units		BPM noise	Calibration errors (%)		$\|\vec{V}\|^2$
Magnet	Component f	average	r.m.s.	(μm)	BPMs	Corr.	
MB	b_2	$+0.00 \pm 0.01$	0.06 ± 0.01				
MB	a_2	-0.04 ± 0.03	0.12 ± 0.02	25	0	0	~ 14600
MB	b_3	$+0.01 \pm 0.21$	0.96 ± 0.15				
MQ	b_2	-0.44 ± 0.26	1.17 ± 0.19				
MB	b_2	$+0.00 \pm 0.01$	0.05 ± 0.01				
MB	a_2	$+0.00 \pm 0.03$	0.11 ± 0.02	50	1	0.1	~ 7200
MB	b_3	$+0.45 \pm 0.20$	0.89 ± 0.15				
MQ	b_2	-0.38 ± 0.26	1.21 ± 0.19				
MB	b_2	$+0.00 \pm 0.01$	0.06 ± 0.01				
MB	a_2	-0.02 ± 0.02	0.08 ± 0.01	100	4	0.2	~ 5500
MB	b_3	$+0.01 \pm 0.22$	1.00 ± 0.15				
MQ	b_2	-0.68 ± 0.38	1.72 ± 0.27				
MB	b_2	$+0.00 \pm 0.01$	0.06 ± 0.01				
MB	a_2	$+0.03 \pm 0.02$	0.10 ± 0.01	200	4	0.2	~ 5000
MB	b_3	$+0.10 \pm 0.19$	1.06 ± 0.14				
MQ	b_2	-0.79 ± 0.34	1.90 ± 0.25				

Table 2: Fit of the b_2, a_2 and b_3 components of the dipoles and of the b_2 components of quadrupoles for different input conditions on noise and calibration errors. The model of the machine used for those simulations included all normal and skew field errors of order two (b_2, a_2) to 5 (b_5, a_5) of the main dipoles and quadrupoles, generated according to error table 9901. 20 seeds were generated for the three first cases, 30 for the last case (noise of 200 μm).

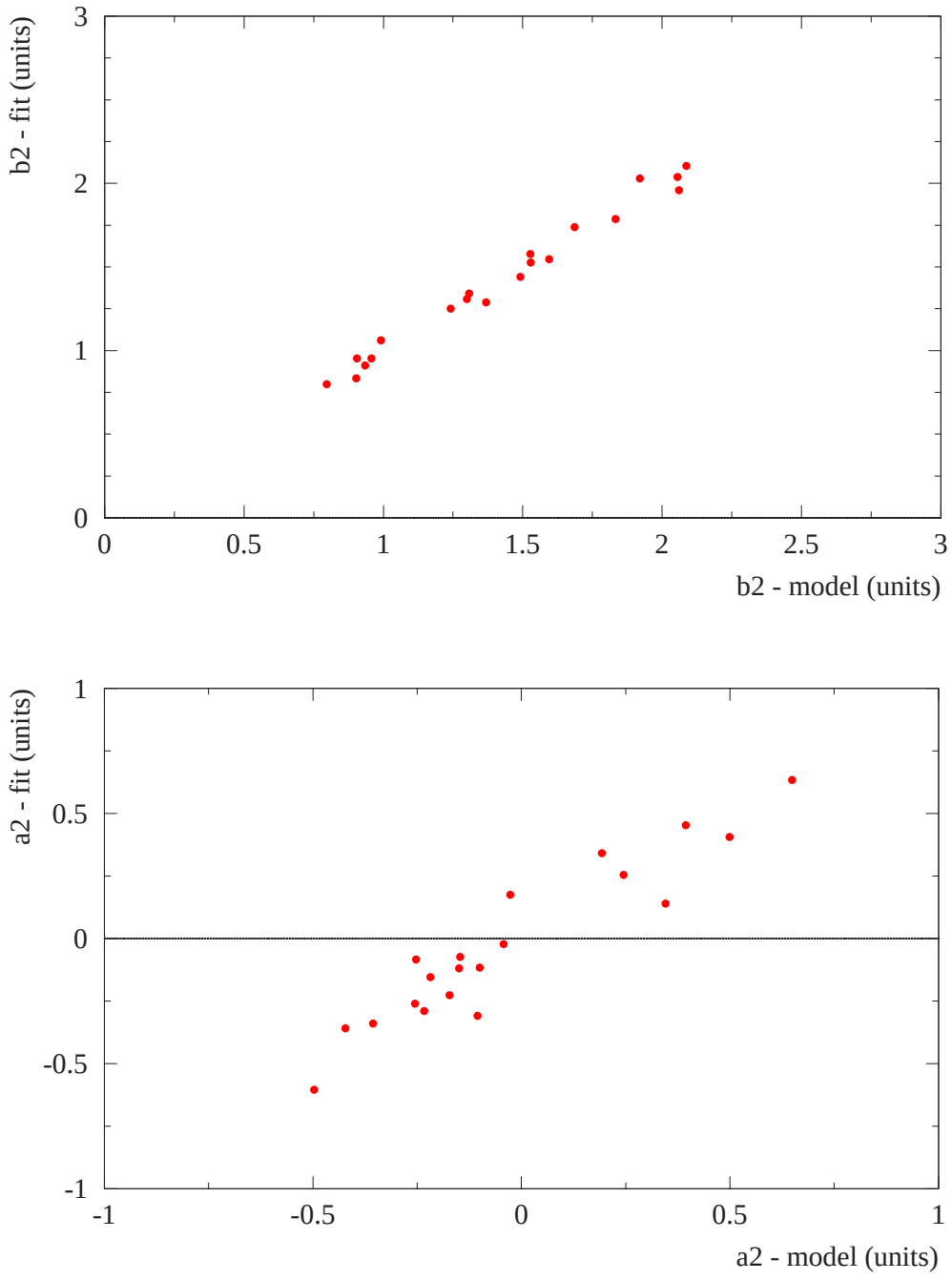

Figure 5: Correlation between the fit result and the simulation input for the average b_2 (top) and a_2 (bottom) field error of the main dipoles.

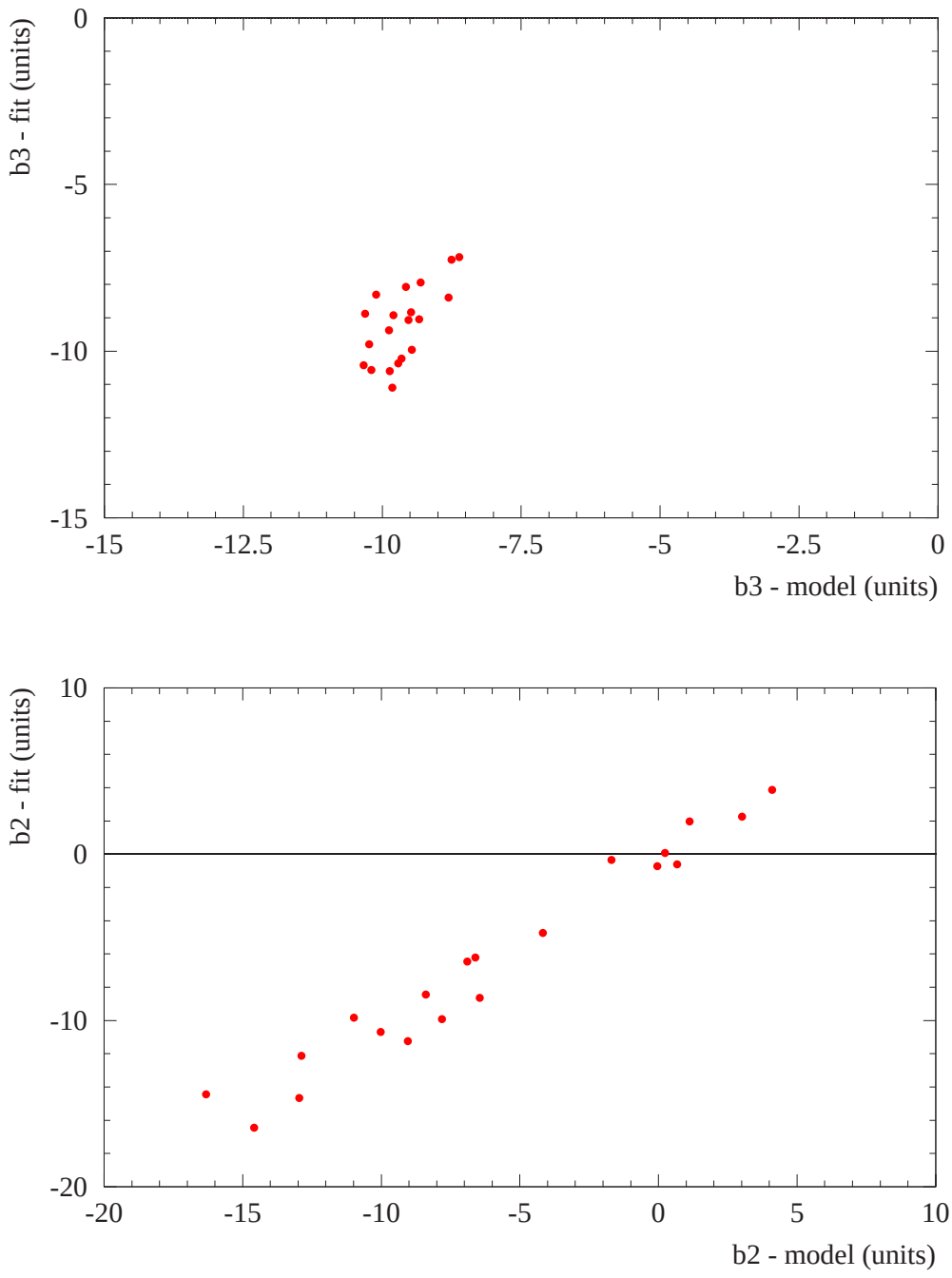

Figure 6: Correlation between the fit result and the simulation input for the average b_3 field error of the main dipoles (top) and for the average b_2 field error of the main quadrupoles (bottom).

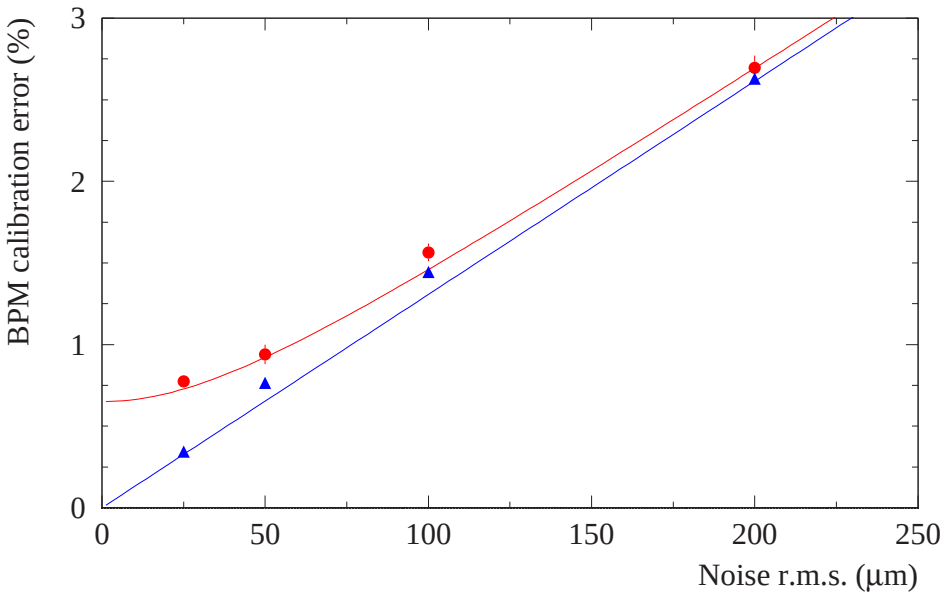

Figure 7: Dependence of the error on the reconstructed BPM calibration on the r.m.s. BPM noise for a machine model with field errors of orders 2 to 5 (•) and for a machine without any field error (▲).

3.6 Monitor and Corrector Calibration

It is also interesting to analyze the reconstructed monitor and orbit corrector calibrations and compare them to the initial input values. The error on the reconstructed BPM calibration is shown in Figure 7 as a function of the monitor noise. For a machine model without any field errors, where the only measurement errors are due to the noise and where no field errors need to be adjusted, the error on the calibration factor scales as expected directly with the monitor noise. For a machine model including systematic and random field errors, the BPM calibrations are biased by the random components of the field errors whose effects are partially absorbed into the calibration factors by the fit. For a machine model including field errors of orders 2 to 5, the additional r.m.s. BPM calibration bias corresponds to $\sim 0.65\%$. A similar observation can be made for the orbit corrector calibration errors shown in Figure 8. In that case the calibration bias due to the random components is $\sim 0.6\%$.

4 Conclusion

The present study of trajectory response study for one LHC arc indicates that for noise conditions of up 200 μm r.m.s., it is possible to determine the average a_2, *btwo* and b_3 field errors of the main dipoles and the average b_2 field error of the main quadrupoles and perform a check of the test bench measurements of the magnets.

In this study the influence of injection errors has not been considered because the LOCO program is presently not able to handle such an additional complication. The conclusions

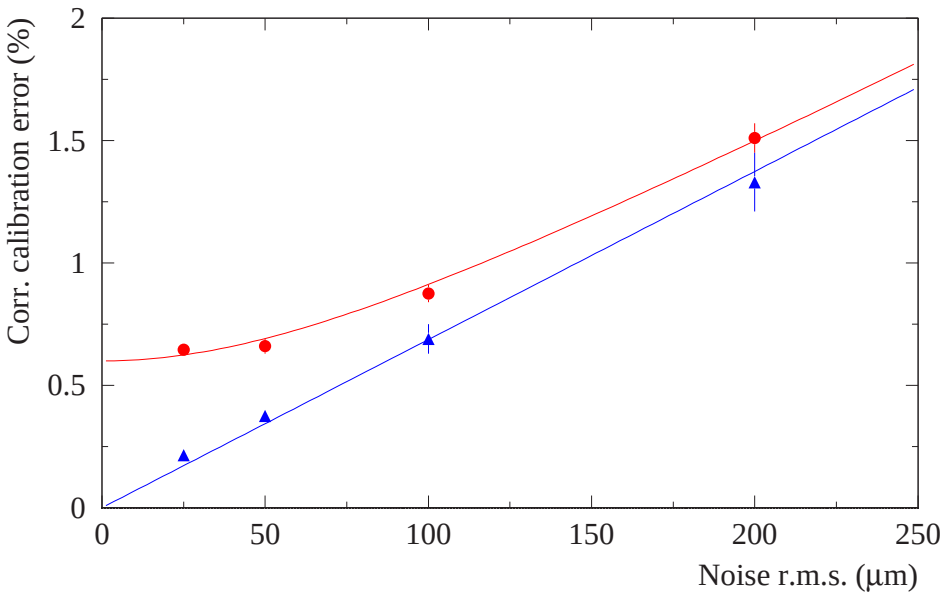

Figure 8: Dependence of the error on the reconstructed orbit corrector calibration on the r.m.s. BPM noise for a machine model with field errors of orders 2 to 5 (•) and for a machine without any field error (▲).

apply therefore only to a situation including injection errors of those errors do not exceed $\sim 200\mu$m, i.e. $\approx 0.2\sigma$. For significantly larger injection errors, it is necessary to either average a large number of injection to average out such errors or to include an injection oscillation into the fit for each trajectory response. The later option requires a significant modification of the LOCO program.

5 Acknowledgements

The author would like to thank J. Safranek for providing the LOCO code and its documentation.

References

[1] J. Safranek, Nucl. Instr. Meth. **A388** (1997) 27.

[2] J. Wenninger, minutes of the SPS Studies Working Group, 11^{th} June 2002.
J. Wenninger, minutes of the SL Operations Comittee meeting, 4^{th} July 2002.

[3] H. Grote and F. Iselin, *The MAD Program*, CERN/SL/90-13 Rev. 5, 1996.

[4] W. Press, B. Flannery, S. Teukolsky and W. Vetterling, *Numerical Recipes* (Cambridge University Press, Cambridge, 1987), 1st ed.

[5] B. Autin and Y. Marti, CERN report ISR MA/73-17, 1973.

[6] Engineering Specification LHC-M-ES-001.00 rev 1.1

[7] O. Brüning and S. Fartoukh, *Field Quality Specification for the LHC Main Dipole Magnets*, LHC Project Report 501 (2001).

[8] R. Jones, *BPM System and expected Performance*, LHC BI Review Workshop, November 2001.
http://sl-div-bi.web.cern.ch/sl-div-bi/Conf&work/LHC-BI-review/agenda.htm